# Effects of anchor placement on mean-CRB for localization

N. Salman, H. K. Maheshwari, A.H. Kemp, M. Ghogho
School of Electronic and Electrical engineering,
University of Leeds.
Leeds LS2 9JT, UK
email: {elns, elhkm, a.h.kemp, m.ghogho@leeds.ac.uk}

***Abstract*—**
**In this paper we discuss the lower bound i.e. the Cramer-rao-bound (CRB) on the accuracy of localization of nodes in a wireless network. We investigate the effects of anchor (or base station) placement on optimal target node positioning. The optimal and worst anchor positions are determined through extended simulation by comparing their mean CRB. Furthermore the ramifications of an additive and multiplicative noise model on the mean CRB are explored. Finally, the least squares (LS) method for localization is used and its performance is compared with the lower bound for optimal anchor positions.**

## I. Introduction

In recent years, there has been a great interest in research towards positioning of wireless devices. Precise and accurate localization is of great importance in military, health, environment, and commercial applications [1]. For outdoor positioning, the global positioning system (GPS) is most widely used, but it exhibits suboptimal performance in harsh propagation environments (i.e. inside buildings, underground and between heavy vegetative cover) due to the absence of a line of sight (LoS). Also, due to the high power requirements of GPS, it has become impractical to employ GPS technology in low power networks such as wireless sensor networks (WSNs). On the other hand, cellular based positioning systems such as the enhanced 911 (E911) have also been recently implemented. With the E911 service, the position of the calling party can be pinpointed in cases when the caller cannot locate itself (e.g. on a remote highway or during a kidnapping).

Two widely used methods for range estimation are the time-of-arrival (ToA) and the received signal strength (RSS). Various techniques have been developed to solve the trilateration distance equations. These include the LS methods [2], the weighted LS method [3] and the maximum likelihood (ML) approach [4]. However the performance of these algorithms is bounded by the CRB. The CRB puts a lower bound on the variance of any unbiased estimator.

The CRB for localization is dependent on the geometry of the anchors and the target node. However the results in [6] are based on the additive noise model (aNm) while a modified CRB based on the multiplicative noise model (mNm) is proposed in [7]. In this paper, we investigate the optimal anchor placement for both models. We begin by giving a review of the two noise models in section-II. In section III we discuss the CRB for localization. Our simulation results are presented in section-IV. In section-V the LS method is simulated and compared with the lower bound, which is followed by the conclusion.

## II. Signal models

Let us consider a network consisting of $N$ anchor nodes whose locations $\theta_i = (x_i, y_i)^T$ for $i = 1, ..., N$ are known, this can be done by placing these anchors at predefined spots or their position can be determined via GPS. It is desired to determine the location of a target node $\theta = (x, y)^T$. Then the estimated distance between each anchor and the target node can be modeled either by the aNm or the mNm. The aNm is a widely accepted signal model, however the

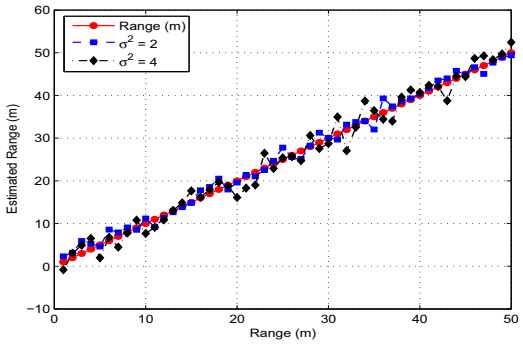


Figure 1. Simulation of estimated range for aNm

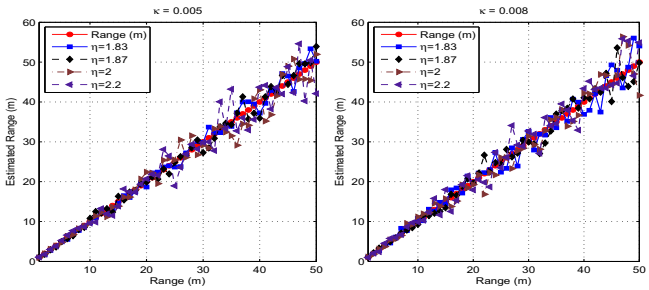


Figure 2. Simulation of estimated range for mNm

mNm is more suitable for practical propagation channels. The two noise models are discussed in the following subsections.

### A. Additive noise model

The signal received at the target node from the $i^{th}$ anchor is given by

$$r_i(t) = A_i s(t - \tau_i) + n_i(t) \tag{1}$$

where $A_i$ is the amplitude or attenuation of the signal, $\tau_i$ is the propagation delay and $n_i(t)$ is the thermal noise. The delay $\tau_i$ that is dependent on the distance between the anchor and the target node is given by

$$\tau_i(x, y, \ell_i) = \frac{1}{c}\sqrt{(x - x_i)^2 + (y - y_i)^2} + \ell_i \tag{2}$$

where $c$ is the speed of the electromagnetic wave $\left(c \simeq 3 \times 10^8\right)$ and $\ell_i$ is non line of sight (NLoS) bias. Since in the present work, we only consider the LoS case, thus $\ell_i = 0$.

From Eq. (2), we note that the distance between $i^{th}$ anchor and the target node is given by

$$d_i = c\tau_i \tag{3}$$

To include distances from $N$ anchors, Eq. (3) is given in vector form:

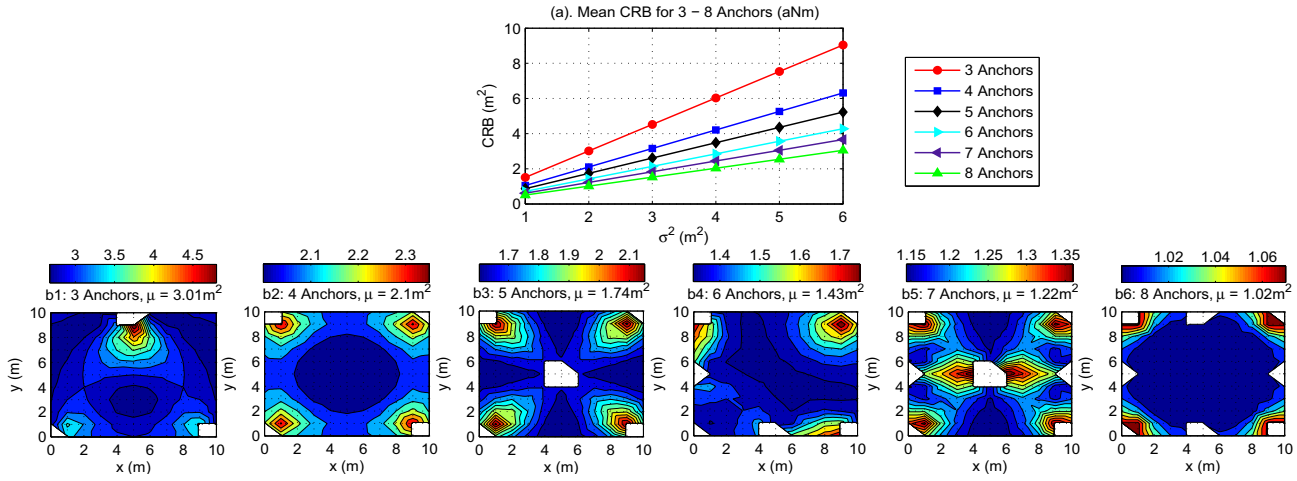


Figure 3. Optimal anchor positions and corresponding CRB for aNm

$$\mathbf{d}(\theta) = [d_1, ..., d_N]^T \tag{4}$$

Thus the estimated distance $\hat{d}_i$ is as follows,

$$\hat{d}_i = d_i + n_i, \tag{5}$$

where $n_i \sim \mathcal{N}\left(0, \sigma_i^2\right)$ is the additive white Gaussian noise with constant standard deviation $\sigma_i$, that is independent of $d_i$.

Similarly, in vector form:

$$\hat{\mathbf{d}} = [\hat{d}_1, ..., \hat{d}_N]^T \tag{6}$$

Fig. 1 shows how the aNm effects the estimated distance or range.

### B. Multiplicative noise model

For the multiplicative noise model we can write Eq. (5) as

$$c\hat{\tau}_i = c\tau_i + cn_i \tag{7}$$

Then the CRB on the variance of the ToA estimate is given as [5]

$$\sigma^2(\hat{\tau}) \geq \frac{1}{8\pi^2\beta^2 SNR} \tag{8}$$

where $\beta$ is the effective bandwidth of the signal and the received power from the $i^{th}$anchor is given by [8]:

$$P_i = P_t \frac{\nu}{d_i^{\eta}} \tag{9}$$

where $\nu$ is the frequency related loss. It is also dependent on antenna heights and other physical layer effects. $P_t$ is the transmit power. $\eta$ is the pathloss exponent (PLE), its value is generally taken between 2 to 5 depending on the type of environment [8]. In a previous work we conducted experiments to estimate the PLE for indoor and outdoor cases [10].

The signal-to-noise ratio (SNR) is hence given by:

$$SNR = \frac{P_i}{N_0} \tag{10}$$

where $N_0$ is the noise power. Putting the value of Eq. (9) in Eq. (10) and then back in Eq. (8), the standard deviation on the estimated distance is given by:

$$\overline{\sigma}_i = \kappa d_i^{\frac{\eta}{2}} \tag{11}$$

where $\kappa = c\sqrt{\frac{N_0}{8\pi^2\beta^2 P_t \vartheta}}$ .

Following the distance dependent variance model, Eq. (7) can be written as

$$\hat{d}_i = d_i + \kappa d_i^{\frac{\eta}{2}}\gamma \tag{12}$$

Here $\gamma$ is Gaussian random variable with zero mean and unit variance. Thus the noise model in Eq. (12) is multiplicative due to the term $d_i^{\frac{\eta}{2}}\gamma$.

The variation in the estimated distance for the mNm is illustrated in Fig. 2.

## III. Cramer-Rao Bound

The accuracy of $\hat{\theta}$ being an unbiased estimate of $\theta$ is bounded by [5]:

$$\text{var}(\hat{\theta}_i) \geq \left[\frac{1}{\mathbf{I}(\boldsymbol{\theta})}\right]_{ii} \tag{13}$$

where $\boldsymbol{\theta} = [\theta_1\theta_2...\theta_p]^T$is the vector parameter to be estimated and $\mathbf{I}(\boldsymbol{\theta})$ is the $p \times p$ Fisher information matrix (FIM) and is defined by [5]

$$[\mathbf{I}(\boldsymbol{\theta})]_{ij} = -E\left[\frac{\partial^2 \ln p(\mathbf{x};\theta)}{\partial\theta_i \partial\theta_j}\right]; i = 1, 2, ..., p; j = 1, 2, ..., p \tag{14}$$

where $p(\mathbf{x};\theta)$ is the likelihood function and E$\{.\}$ refers to the expected value and is taken w.r.t $p(\mathbf{x};\theta)$. The derivatives are taken at the true value of $\theta$.

The FIM for the aNm model is given by [6]

$$\mathbf{I}(\theta) = \begin{bmatrix} \sum_{i=1}^{N} \frac{(x-x_i)^2}{\sigma_i^2 d_i^2} & \sum_{i=1}^{N} \frac{(y-y_i)(x-x_i)}{\sigma_i^2 d_i^2} \\ \sum_{i=1}^{N} \frac{(y-y_i)(x-x_i)}{\sigma_i^2 d_i^2} & \sum_{i=1}^{N} \frac{(y-y_i)^2}{\sigma_i^2 d_i^2} \end{bmatrix}$$

where $\alpha_i$ being the angle of the target node with the $i^{th}$anchor.

The FIM for the mNm is given by [7]

$$\mathbf{I}(\theta) = \begin{bmatrix} \sum_{i=1}^{N} \frac{\upsilon_i \cos^2(\alpha_i)}{\overline{\sigma}_i^2} & \sum_{i=1}^{N} \frac{\upsilon_i \cos(\alpha_i)\sin(\alpha_i)}{\overline{\sigma}_i^2} \\ \sum_{i=1}^{N} \frac{\upsilon_i \cos(\alpha_i)\sin(\alpha_i)}{\overline{\sigma}_i^2} & \sum_{i=1}^{N} \frac{\upsilon_i \sin^2(\alpha_i)}{\overline{\sigma}_i^2} \end{bmatrix} \tag{15}$$

where $\upsilon_i = 1 + \frac{\beta^2\kappa}{2} d_i^{\beta-2}$, which is distance dependent. Since the lower bounds in both noise models are a function of the geometry of the anchors and the target node, it is obvious that certain anchor locations would offer better accuracy than others. These optimal anchor locations are discussed in the next section.

## IV. Optimal anchor positions

The estimation of different target node positions are subject to different accuracies. We aim to find anchor locations that would give us an overall best accuracy for all target positions. Thus we choose the anchors that offers the minimum of the mean CRB. In the following subsection, we discuss these optimal anchor locations.

### A. Optimal anchor positions for aNm

Trilateration in a 2-D case requires a minimum of three anchor nodes. Individual distance between each anchor and the target node is represented by a circle or line of position (LoP). The point of intersection of these circles is the target node location. In order to

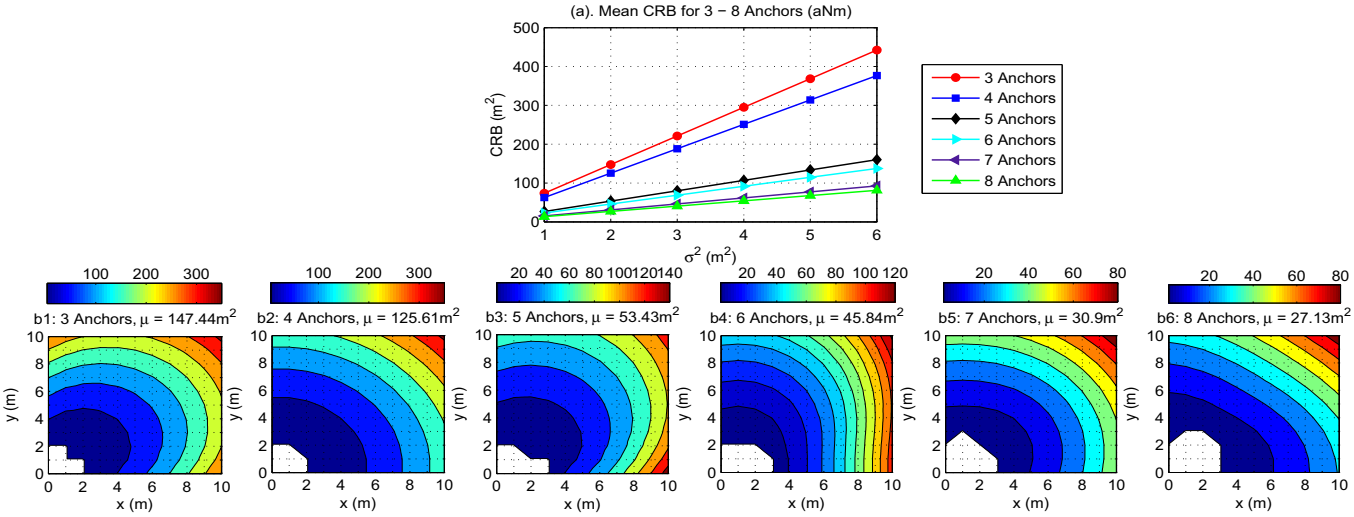


Figure 4. Poor anchor positions and corresponding CRB for aNm.

get an insight on how the lower bound is affected by the relative angle between the target and the anchor node, the CRB for every point in a 10x10 2-D plane is calculated for fixed anchor positions. Furthermore, in order to achieve the anchor positions that give the minimum mean CRB, all the combinations of anchors are taken. i.e. $C_r^n = \frac{n!}{r!(n-r)!}$, where $n$ is the dimension of the area and $r$ is the number of anchors. As an example, in our case an area of 10x10 is taken for case (b1) in Fig.3, where 3 anchors are employed, we get a total combination of 161,700 anchor positions. It is well known that when all anchors are placed along the same line ($x$ or $y$ coordinates being the same), then the variance of the CRB rises to infinity and in such cases positioning algorithms such as the LS fail to estimate the target node's coordinates. Thus in order to avoid this problem, all the collinear anchor positions are not considered in our simulations. The number of such combination is given by $x^{'} * C_r^{x^{'}} + y^{'} * C_r^{y^{'}}$ , where $x', y'$ represent the lengths of $x$ and $y$ coordinates respectively. For case (b1) in Fig. 3, a total of 2,400 collinear anchor positions are avoided.

Fig. 3 shows the optimal anchor positions for 3-8 anchors. The contour plots Fig. 3 (b1-b6) are obtained for a constant variance for all cases i.e $\sigma_i = \sigma = 2$. It is observed that when only 3 anchors are placed in a square area, the highest accuracy in the estimated location is achieved when the trio is placed at the corners of an equilateral triangle. This triangle is of maximum size as 2 anchors are placed at the corners of one side of the square area while the $3^{rd}$ anchor is placed at the center of the opposite side. It is also noted that the bound increases as the target node goes near any of the anchor nodes. The best location for 4 anchors is at the corners of the square area while the best location for an additional 5th anchor is the center of the area. Similarly such symmetrical anchor locations are exhibited in Fig 3 (b4-b6) where 6, 7 and 8 anchors are used. The white points in the figures show the anchor locations where the target node placement is avoided. It should be noted that these configurations are independent of rotation i.e. the same results are obtained if the entire set of anchors are simultaneously rotated clockwise or counter-clock wise by $90°$or $180°$. Fig. 3a displays the mean CRB as a function of variance. It is noted that as the number of anchors increase the variance effect on the mean CRB becomes smaller.

Fig. 4 (b1-b6) illustrates the anchor locations which exhibits the worst localization accuracy and which gives the maximum mean CRB. It is observed that the variance of the estimator is the highest if all the anchors are placed in the same corner of a square area. It is also seen in Fig. 4a that the improvement in performance is negligible if the number of anchors is increased from 5 to 8 for such a poor network geometry. Furthermore, it is evident from both Fig. 3 and 4 that when the minimum 3 anchors are placed optimally (with mean CRB = 1.5063 and 9.0379 for $\sigma^2 = 1 \text{ and } 6$), it out performs a poor deployment of 8 anchors (mean CRB = 13.562 and 81.375 for $\sigma^2 = 1 \text{ and } 6$).

### B. Optimal anchor positions for mNm

The plot in Fig. 6a illustrates the mNm mean CRB as a function of the number of anchor nodes placed at the optimal positions for the aNm. The contour plot for $\kappa = 0.001$ and $\eta = 4$ is given in Fig. 6 (b1-b6). The mean CRB for the mNm is lower than the aNm for anchors 5 and more. However this is not true for all values of $\kappa$ and $\eta$. The optimal anchor placement for mNm is different than the aNm, as shown in Fig 5 (a1-a3) for 3, 4 and 5 anchors. However, these optimal placements depend on the actual scale of the area, the constant $\kappa$ and $\eta$. The mNm CRB becomes lower as values of $\kappa$ and $\eta$ are decreased. While both CRB's are almost identical for $\eta = 2$. In a dense urban environments where $\eta$ =4 to 5 [8] or highly cluttered indoor scenarios, the mNm is a more suitable noise model. In such cases, results from Fig. 5 suggest that it is not always optimal to place the anchor nodes at the corners as in Fig. 3. In fact, the optimality can not even be guaranteed by the anchor placement in Fig. 5 as they are for a particular dimension and for an assumed value of $\kappa$ and $\eta$. Thus, for the mNm case, the values of $\kappa$ and $\eta$ need to be obtained experimentally before anchor deployment. Finally, the worst anchor placement for mNm is similar as that for aNm i.e all anchors are placed at one corner of the area.

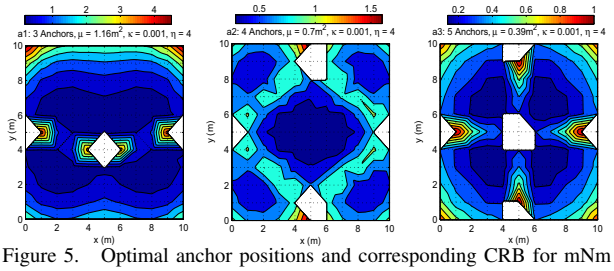


Figure 5. Optimal anchor positions and corresponding CRB for mNm

## V. Performance of Least Squares (LS) Method at Optimal Anchor Positions

In this section we compare the performance of the LS method for position estimation with the mean CRB for optimal anchor placement.

The elements of the vector $\hat{\mathbf{d}}$ in Eq. (6) are given by

$$\hat{d}_i = \sqrt{(x - x_i)^2 + (y - y_i)^2}$$

where $\hat{d}_i$ represent the noisy estimated distances and the circles obtained from them do not intersect at a common point.

In order to solve the LS problem (which is non-linear) for $(x, y)$ coordinates, the distance equation of the $r^{th}$ anchor is fixed and all other distance equations are subtracted from it, yielding [9]:

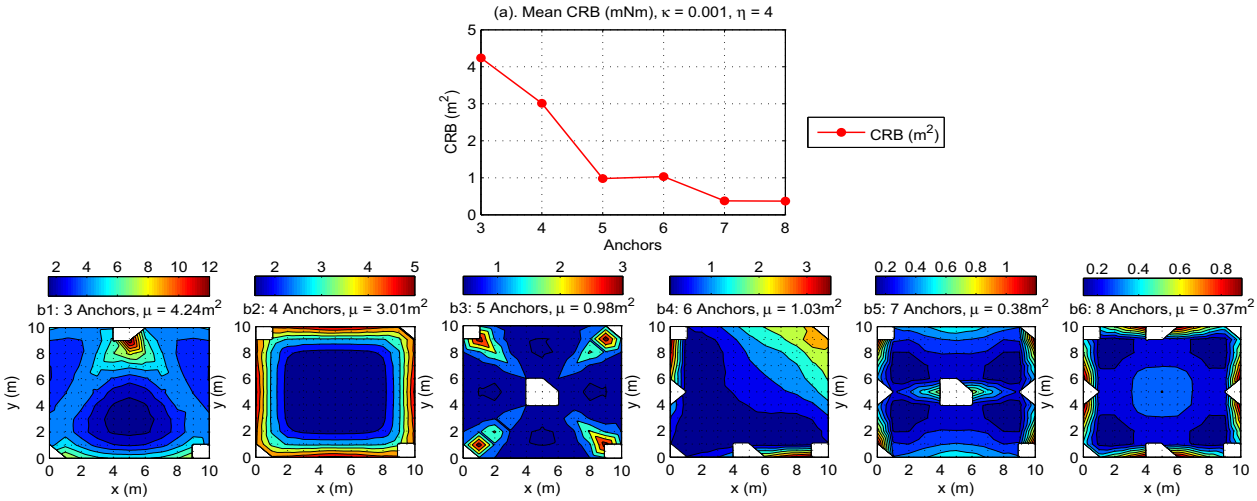


Figure 6. Suboptimal anchor positions and corresponding CRB for mNm

$$x_i^2 - x_r^2 + y_i^2 - y_r^2 - 2xx_i + 2xx_r - 2yy_i + 2yy_r = \hat{d}_i^2 - \hat{d}_r^2 \quad (16)$$

for $i = 1...N$, $i \neq r$ and where $K_{i,r} = x_{i,r}^2 + y_{i,r}^2$

Similarly, in matrix form $\mathbf{A}\theta = \frac{1}{2}\mathbf{b}$, where

$$\mathrm{A} = \begin{bmatrix} x_1 - x_r & y_1 - y_r \\ x_2 - x_r & y_2 - y_r \\ \vdots & \vdots \\ x_N - x_r & y_N - y_r \end{bmatrix}, \mathbf{b} = \begin{bmatrix} K_1 - K_r + \hat{d}_r^2 - \hat{d}_1^2 \\ K_2 - K_r + \hat{d}_r^2 - \hat{d}_2^2 \\ \vdots \\ K_N - K_r + \hat{d}_r^2 - \hat{d}_N^2 \end{bmatrix} \quad (17)$$

and the estimated coordinates of the target node is given by the vector $\widetilde{\theta} = \left(\mathbf{A}^T\mathbf{A}\right)^{-1}\mathbf{A}^T\mathbf{b}$. The mean square error (MSE) is given by: $\mathbf{MSE} = \mathrm{Tr}\left(\mathbf{E}\{(\widetilde{\theta} - \theta)(\widetilde{\theta} - \theta)^{\mathbf{T}}\}\right)$,where Tr(.) represents the trace of the matrix. Fig. 7(a) compares the MSE of the LS method with the mean CRB for optimal anchor positions. Fifty iterations are taken for each range measurement while the variance is incremented from 1 to 4 for aNm. The MSE for all target locations is computed and its mean is compared with the mean CRB. The simulation uses the same setup of a 10x10 2-D plane as in the previous case. It is seen that although the number of anchors are increased from 4 to 5, it does not have a significant impact on the accuracy. Fig. 7(b) compares the MSE of LS for mNm with the mean CRB for $\eta = 4$. The right $y$ axis of Fig. 7 (b) shows the mean MSE of the LS method. It is observed that error is colossal for $\eta = 4$. The effect of the different values of $\eta$ is illustrated in Fig. 8, where the LS method for $\eta = 2$ and 3 are simulated. As can be seen the LS offers less error for a smaller value of $\eta$.

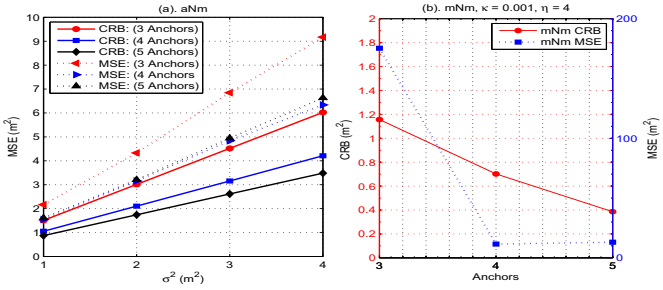


Figure 7. Performance of the LS method for aNm and mNm at optimal anchor placement and comparison with CRB

## VI. Conclusions

In this paper, the impact of anchor positions on the localization of nodes was discussed. Based on our extensive simulations, optimal anchor location for both aNm and mNm have been achieved. It is evident from the simulations that for an aNm the CRB decreases as the target node is moved away from the anchors. Thus in a square area the the lowest accuracy is observed near the anchor while the highest accuracy is achieved at the center of the area. On the other hand, for highly cluttered environments where the $\eta$ value of 4-5 is taken, the mNm is more suitable. In such scenarios, the minimum mean CRB is not offered by anchors placed at the corners of a square area. Optimal anchor placement in mNm depends on the dimension of the area and the value of $\eta$ and $\kappa$.

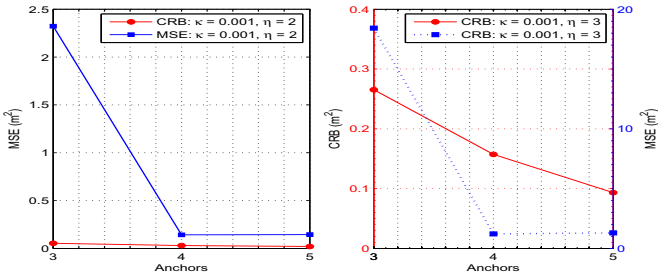


Figure 8. Performance of the LS method for 3, 4 and 5 anchors for $\eta = 2$ and 3

## References


[1] James J. Caffery, "Wireless Location in CDMA Cellular Radio Systems",Kluwer Academic Publishers-ISBN:0792377036

[2] J. J. Caffery, "A new approach to the geometry of TOA location," in Proc. IEEE Veh. Technol. Conf. (VTC), vol. 4, Boston, MA, Sep. 2000, pp. 1943–1949.J. J. Caffery, "A new approach to the geometry of TOA location," in Proc. IEEE Veh. Technol. Conf. (VTC), vol. 4, Boston, MA, Sep. 2000, pp. 1943–1949.

[3] S. Gezici and Z. Sahinoglu, "UWB geolocation techniques for IEEE 802.15.4a personal area networks," MERL Technical report, Cambridge, MA, Aug. 2004.

[4] Y. T. Chan, H. Y. C. Hang, and P. C. Ching, "Exact and approximate maximum likelihood localization algorithms," IEEE Trans. Veh. Technol., vol. 55, no. 1, pp. 10–16, Jan. 2006.

[5] S. M. Kay, Fundamentals of Statistical Signal Processing: Estimation Theory. Upper Saddle River, NJ: Prentice Hall, Inc., 1993.

[6] C. Cheng and A. Sahai, "Estimation bounds for localization," in Proc. IEEE Int. Conf. Sensor and Ad-Hoc Communications and Networks (SECON), Santa Clara, CA, Oct. 2004, pp. 415–424.

[7] Tao Jia; Buehrer, R.M.; , "A new Cramer-Rao lower bound for TOA-based localization," Military Communications Conference, 2008. MILCOM 2008. IEEE , vol., no., pp.1-5, 16-19 Nov. 2008 doi: 10.1109/MILCOM.2008.4753258.

[8] S. Haykin, M.Moher, "Modern Wireless Communications". Pearson Prentice Hall, 2005 ISBN 0130224723.

[9] Guvenc, I.; Chia-Chin Chong; Watanabe, F.; , "Analysis of a Linear Least-Squares Localization Technique in LOS and NLOS Environments," Vehicular Technology Conference, 2007. VTC2007-Spring. IEEE 65th , vol., no., pp.1886-1890, 22-25 April 2007.

[10] Maheshwari, H.K., Kemp, A.H, "On the Enhanced Ranging Performance for IEEE 802.15.4 Compliant WSN Devices", Third International workshop on Wireless Sensor Networks - theory and practice (WSN'2011), Feb 2011, Paris, France.